

Ultrafast Fluorescence Detection in Tris(2,2'-bipyridine)ruthenium(II) Complex in Solution: Relaxation Dynamics Involving Higher Excited States

Achikanath C. Bhasikuttan,^{*,†} Masaya Suzuki, Satoru Nakashima, and Tadashi Okada^{*,‡}

Contribution from the Department of Chemistry, Graduate School of Engineering Science, Osaka University, Toyonaka, Osaka 560-8531, Japan

Received March 8, 2002

Abstract: The excited-state dynamics of a transition metal complex, tris(2,2'-bipyridine)ruthenium(II), [Ru(bpy)₃]²⁺, has been investigated using femtosecond fluorescence upconversion spectroscopy. The relaxation dynamics in these molecules is of great importance in understanding the various ultrafast processes related to interfacial electron transfer, especially in semiconductor nanoparticles. Despite several experimental and theoretical efforts, direct observation of a Franck-Condon excited singlet state in this molecule was missing. In this study, emission from the Franck-Condon excited singlet state of [Ru(bpy)₃]²⁺ has been observed for the first time, and its lifetime has been estimated to be 40 ± 15 fs. Biexponential decays with a fast rise component observed at longer wavelengths indicated the existence of more than one emitting state in the system. From a detailed data analysis, it has been proposed that, on excitation at 410 nm, crossover from higher excited ¹(MLCT) states to the vibrationally hot triplet manifold occurs with an intersystem crossing time constant of 40 ± 15 fs. Mixing of the higher levels in the triplet state with the singlet state due to strong spin-orbit coupling is proposed. This enhances the radiative rate constant, *k_r*, of the vibrationally hot states within the triplet manifold, facilitating the upconversion of the emitted photons. The vibrationally excited triplet, which is emissive, undergoes vibrational cooling with a decay time in the range of 0.56–1.3 ps and relaxes to the long-lived triplet state. The results on the relaxation dynamics of the higher excited states in [Ru(bpy)₃]²⁺ are valuable in explaining the role of nonequilibrated higher excited sensitizer states of transition metal complexes in the electron injection and other ultrafast processes.

Introduction

Understanding the excited-state dynamics of transition metal complexes is extremely important in an application which has shown an upsurge over the past decade, namely, sensitization of wide band gap semiconductors to achieve solar energy conversions.^{1–8} Sensitizers based on metal complexes, especially Ru(dcbp)₂(CNS)₂ (where dcbp is 4,4'-dicarboxylic-2,2'-bipyridine, popularly known as RuN3 dye), have been most successful in sensitizing TiO₂ to achieve the highest conversion efficiency

of the dye-sensitized solar cells, and this has given impetus to research directed to understanding the photophysical aspects of many ruthenium-based metal complexes.³ In solar energy applications, the sensitizer dye is excited with visible light to the electronic excited state. If this state is energetically above the conduction band edge of the semiconductor, electron injection into the conduction band can occur. Such fast electron transfer is the primary step in charge separation and subsequent energy conversion in dye-sensitized solar cells.¹ It has been widely accepted that higher energy conversion efficiency results from a fast electron injection from the sensitizer dye to the semiconductor and a much slower back electron transfer to the sensitizer. Recent reports employing ultrafast transient absorption measurements in the visible, near-IR, and mid-IR regions suggested that the electron injection process from RuN3 dye to nanocrystalline TiO₂ film occurs in <100 fs.^{9–13} Direct observa-

* To whom correspondence should be addressed. E-mail: okada@chem.es.osaka-u.ac.jp.

† Permanent address: Radiation Chemistry and Chemical Dynamics Division, Bhabha Atomic Research Centre, Mumbai, India. E-mail: bkac@apsara.barc.ernet.in.

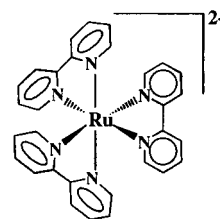
‡ Tel.: (+81) 6 6850 6240. Fax: (+81) 6 6850 6244. E-mail: okada@chem.es.osaka-u.ac.jp.

- (1) Miller, R. J. D.; McLendon, G. L.; Nozik, A. J.; Schmickler, W.; Willig, F.; *Surface Electron-Transfer Processes*; VCH: New York, 1995.
- (2) Hagfeldt, A.; Grätzel, M. *Chem. Rev.* **1995**, *95*, 49.
- (3) Grätzel, M. *Heterogeneous Photochemical Electron Transfer*; CRC Press: Boca Raton, FL, 1988.
- (4) Kalyanasundaram, K.; Grätzel, M. *Coord. Chem. Rev.* **1998**, *177*, 347.
- (5) O'Regan, B.; Grätzel, M. *Nature* **1991**, *353*, 737.
- (6) (a) Bard, A. J. *Science* **1980**, *207*, 139. (b) Bard, A. J.; Fox, M. A. *Acc. Chem. Res.* **1995**, *28*, 141.
- (7) Heller, A. *Acc. Chem. Res.* **1981**, *14*, 154.
- (8) Gerischer, H. *Electrochim. Acta* **1990**, *35*, 1677.

- (9) Asbury, J. B.; Ellingson, R. J.; Ghosh, H. N.; Ferrere, S.; Nozik, A. J.; Lian, T. *J. Phys. Chem. B* **1999**, *103*, 3110.
- (10) Ellingson, R. J.; Asbury, J. B.; Ferrere, S.; Ghosh, H. N.; Sprague, J. R.; Lian, T.; Nozik, A. J. *J. Phys. Chem. B* **1998**, *102*, 6455.
- (11) Hannappel, T.; Burfeindt, B.; Storck, W.; Willig, F. *J. Phys. Chem. B* **1997**, *101*, 6799.
- (12) Tachibana, Y.; Haque, S. A.; Mercer, I. P.; Durrant, J. R.; Klug, D. R. *J. Phys. Chem. B* **2000**, *104*, 1198.

tion of the electron released into the conduction band of TiO_2 showed that the electron injection process is biexponential, and lifetimes of 50 ± 25 fs (84%) and 1.7 ± 0.5 ps (<16%) have been reported.^{9,10} Hannappel et al. have reported a time constant of <25 fs for the electron injection from RuN3 to colloidal anatase TiO_2 film.¹¹ In a recent article on electron injection from RuN3 to TiO_2 nanocrystalline film, Benko et al. reported rapid electron transfer from the nonthermalized singlet excited state, prior to any relaxation process.¹³ Tachibana et al., by employing three different sensitizer dyes on TiO_2 , concluded that the singlet/triplet character of the dye excited state is not critical to the electron injection process.¹² Despite many reports on this topic, the exact origin of the injected electron and time scales of electron injection remain topics of heated debate.¹⁴ The observed electron injection time in these systems appears to be similar to or faster than the typical time of intramolecular vibrational energy redistribution and intersystem crossing in the excited states.^{11,12} Ferrere and Gregg have observed band-selective sensitization in $\text{Fe}(\text{dcbp})_2(\text{CN})_2$ dye adsorbed on TiO_2 and suggested the involvement of electron injection from higher lying excited states.¹⁵ Recently, Iwai et al. have observed stimulated emission from the ¹(MLCT) state of RuN3 dye adsorbed on SnO_2 nanocrystalline thin film under an external applied bias.¹⁶ More recently, Lenzmann et al. have provided a strong indication of the involvement of electron injection from higher excited states of the sensitizer dye molecule by employing surface photovoltage spectroscopy.¹⁷ In short, understanding the relaxation dynamics of the higher excited levels of the sensitizer molecule is crucial in controlling the rate of electron injection processes from the transition metal complexes and has important consequences in a variety of areas ranging from design principles for electron-transfer assemblies to photochemical energy storage devices.

As mentioned above, ruthenium bipyridyl complexes have attracted interest for their photochemical properties due to their wide range of applications, especially as the most efficient sensitizer for dye-sensitized solar energy conversions.³ Owing to the synthetic flexibility to accommodate tailor-made chromophores, transition metal complexes find interest from synthetic, electrochemical, photochemical, and photophysical viewpoints.¹⁸ One kind, tris(2,2'-bipyridine)ruthenium(II), $[\text{Ru}(\text{bpy})_3]^{2+}$, has been considered as a prototype of a wide class of transition metal complexes whose study has formed the basis for the most transition-metal-based photochemical applications.^{19–24}



Tris-(2,2'-bipyridine)ruthenium(II)

Transition metal complexes, $[\text{Ru}(\text{bpy})_3]^{2+}$ in particular, exhibit charge-transfer transitions between the metal-centered d orbital and the ligand-centered π^* orbital, commonly known as metal-to-ligand charge-transfer (MLCT) transitions. One of the interesting aspects involves the nature of the MLCT state, specifically whether the excited electron is localized on one of the three bipyridyl ligands or delocalized over all three bipyridyl units.^{25–29} Though it is widely accepted that on excitation, the electron is localized on one of the bipyridine rings, the history before the localization of the electron remains a topic of hot debate.^{25,30} On optical excitation, such localization creates a large dipole moment in the excited state (~ 14 D), which is oriented along the axis from the metal to the center of one of the bipyridine moieties.³¹ Since solvent plays an important role in the solvation of the nascent excited dipole, such systems also provide a convenient platform for examining how solvation dynamics is coupled to the photoinduced charge-transfer events. Femtosecond time-resolved anisotropy measurements have revealed solvent-dependent anisotropy decay in different nitrile solutions.³⁰ This has been attributed to initial delocalization of the excited electron over all three ligands, followed by charge localization onto a single ligand.³⁰ From the ultrafast nature of these processes, it has been proposed that the localization process is coupled to the nondiffusive solvation dynamics.

The excited-state properties of $[\text{Ru}(\text{bpy})_3]^{2+}$ have been studied extensively, and the properties of its lowest energy triplet state are fairly well known. Femtosecond pump–probe measurements on the evolution of triplet–triplet absorption have provided 100 fs time constant for the formation of the triplet state.^{30,32} Despite several experimental (vide infra) and theoretical^{26,33} efforts to unravel the intriguing photophysics of this molecule, information on the excited-state dynamics of $[\text{Ru}(\text{bpy})_3]^{2+}$ by direct observation of the Franck–Condon (FC) singlet excited state was missing. It is believed that the ¹(MLCT) state is almost nonfluorescent and that the formation of the ³(MLCT) state is rapid, with a quantum yield near unity.³⁴ The observed emission

(13) Benko, G.; Kallioinen, J.; Korppi-Tommola, J. E. I.; Yartsev, A. P.; Sundstrom, V. *J. Am. Chem. Soc.* **2002**, *124*, 489.

(14) (a) Fessenden, R. W.; Kamat, P. V. *J. Phys. Chem.* **1995**, *99*, 12902. (b) Burfeindt, B.; Hannappel, T.; Storck, W.; Willig, F. *J. Phys. Chem.* **1996**, *100*, 16463. (c) Hilgendorff, M.; Sundstrom, V. *J. Phys. Chem. B* **1998**, *102*, 10505. (d) Martini, I.; Hodak, J. H.; Hartland, G. V. *J. Phys. Chem. B* **1998**, *102*, 9508.

(15) Ferrere, S.; Gregg, B. A. *J. Am. Chem. Soc.* **1998**, *120*, 843.

(16) Iwai, S.; Hara, K.; Murata, S.; Katoh, R.; Sugihara, H.; Arakawa, H. *J. Chem. Phys.* **2000**, *113*, 3366.

(17) Lenzmann, F.; Krueger, J.; Burnside, S.; Brooks, K.; Grätzel, M.; Gal, D.; Ruhle, S.; Cahen, D. *J. Phys. Chem. B* **2001**, *105*, 6347.

(18) Balzani, V.; Juris, A.; Venturi, M.; Campagna, S.; Serroni, S. *Chem. Rev.* **1996**, *96*, 759 and references therein.

(19) Roundhill, D. M. *Photochemistry and Photophysics of Metal Complexes*; Plenum Press: New York, 1994; Chapter 5, p 165.

(20) Juris, A.; Balzani, V.; Barigelli, F.; Campagna, S.; Belsler, P.; Von Zelewsky, A. *Coord. Chem. Rev.* **1988**, *84*, 85.

(21) Petersen, J. D.; Gahan, S. L.; Rasmussen, S. C.; Ronco, S. E. *Coord. Chem. Rev.* **1994**, *132*, 15.

(22) Zang, L.; Rodgers, M. A. J. *J. Phys. Chem. B* **2000**, *104*, 468.

(23) Ogawa, M.; Nakamura, T.; Mori, J.; Kuroda, K. *J. Phys. Chem. B* **2000**, *104*, 8554.

(24) Ikeda, N.; Yoshimura, A.; Tsushima, M.; Ohno, T. *J. Phys. Chem. A* **2000**, *104*, 6158.

(25) Waterland, M. R.; Kelley, D. F. *J. Phys. Chem. A* **2001**, *105*, 4019.

(26) Damrauer, N. H.; Weldon, B. T.; McCusker, J. K. *J. Phys. Chem. A* **1998**, *102*, 3382.

(27) Damrauer, N. H.; Boussie, T. R.; Devenney, M.; McCusker, J. K. *J. Am. Chem. Soc.* **1997**, *119*, 8253.

(28) Braun, D.; Huber, P.; Wudy, J.; Schmidt, J.; Yersin, H. *J. Phys. Chem.* **1994**, *98*, 8044.

(29) (a) Malone, R. A.; Kelley, D. F. *J. Chem. Phys.* **1991**, *95*, 8970. (b) Cooley, L. F.; Bergquist, P.; Kelley, D. F. *J. Am. Chem. Soc.* **1990**, *112*, 2612.

(30) Yeh, A. T.; Shank, C. V.; McCusker, J. K. *Science* **2000**, *289*, 935.

(31) Kober, E. M.; Sulivan, B. P.; Meyer, T. *J. Inorg. Chem.* **1984**, *23*, 2098.

(32) Damrauer, N. H.; Cerullo, G.; Yeh, A.; Shank, C. V.; McCusker, J. K. *Science* **1997**, *275*, 54.

(33) Zheng, K.; Wang, J.; Shen, Y.; Kuang, D.; Yun, F. *J. Phys. Chem. A* **2001**, *105*, 7248.

(34) (a) Demas, J. N.; Adamson, A. W. *J. Am. Chem. Soc.* **1971**, *93*, 1800. (b) Demas, J. N.; Crosby, G. A. *J. Am. Chem. Soc.* **1971**, *93*, 2841. (c) Demas, J. N.; Taylor, D. G.; *Inorg. Chem.* **1979**, *18*, 3177.

from the complex is believed to be from the long-lived $^3(\text{MLCT})$ state.^{35–37} Hence, research on radiative transition in these complexes in liquid media has been mainly centered around the $^3(\text{MLCT})$ state.^{35,37,38} In this process, a wealth of information is lost while the system evolves from the FC singlet state to the emissive $^3(\text{MLCT})$ state. This is where time-resolved fluorescence detection becomes relevant and the femtosecond fluorescence upconversion method provides a sensitive tool to explore such systems.³⁹ While the emissive photon flux from the organic fluorophore is often sufficient to achieve a good signal in fluorescence upconversion measurements, the radiative flux from the triplet state of the bipyridyl complexes is lesser by a factor of 10^3 [the lifetime of the $^3(\text{MLCT})$ state is of the order of several hundreds of nanoseconds] and is not enough to generate sufficient upconverted signal.³⁸ In other words, the FC singlet state is very short-lived, and emission from it, if it occurs, would have a lifetime of a few hundred femtoseconds and could be enough to generate the upconversion signal in the femtosecond time domain. Such an interesting and promising situation led us to explore this system in detail with the fluorescence upconversion method.

It is clear from the above discussion that information on the $^1(\text{MLCT})$ state is most desirable to account for some of these ultrafast processes, and to our knowledge, no attempt has been made to explore the $^1(\text{MLCT})$ emission in the $[\text{Ru}(\text{bpy})_3]^{2+}$ and related complexes. In this paper, we present the details of the femtosecond time-resolved fluorescence emission detected for the first time from the Franck–Condon singlet excited state of $[\text{Ru}(\text{bpy})_3]^{2+}$ by upconversion spectroscopy. On excitation by 410 nm pulses, the system displayed fluorescence emission from nonequilibrated higher excited states having a fast decay constant of 40 ± 15 fs. Fast intersystem crossing involving higher excited states has been proposed to populate the higher vibrational levels in the triplet manifold. Emission from these vibrational hot bands in the triplet manifold displayed lifetimes in the range of 0.56–1.3 ps in the different solvents studied. The results provide strong support to the recent reports suggesting the involvement of a higher excited state in the electron injection process and the give direct evidence of the wavelength-dependent photophysics argued for band-selective sensitization on the semiconductor nanoparticles.^{13,15,17}

Experimental Section

$[\text{Ru}(\text{bpy})_3]^{2+}$ (chloride salt) (Aldrich Chemical Co.) was recrystallized from an acetonitrile/toluene mixture.⁴⁰ All solvents were purchased from Wako Chemicals, Japan (purity better than 99.5%), and were used as received. Steady-state absorption and fluorescence spectra were recorded on a Hitachi U-3500 spectrophotometer and a Hitachi 850E fluorimeter, respectively.

Fluorescence decays were measured by using a fluorescence up-conversion setup. Briefly, the system employs an Ar^+ -pumped femtosecond mode-locked Ti:sapphire system (Tsunami, 70 fs, Spectra Physics), giving ~ 600 mW at ~ 800 nm with a repetition rate of 82 MHz. The second harmonic (SH) output was generated in a 0.8 mm BBO crystal (Type I) separated from the fundamental by a harmonic

separator and was focused by a 40 mm lens onto a sample cell of 1 mm path length for excitation. The polarization of the excitation beam was varied by introducing a half-wave plate in the pump beam and generally was kept at the magic angle (54.7°) with respect to the gate pulse polarization. The emission was collected and collimated by a 1 in. off-axis parabolic mirror (25 mm at 90°) and focused onto a 0.5 mm sum frequency generation (SFG) crystal (Type I) by another off-axis parabolic mirror (200 mm at 90°). The residual fundamental gate pulse, after traversing a variable delay stage, was also focused onto the SFG crystal by a 200 mm lens. The angle between the two beams was held at $\sim 10^\circ$ to achieve maximum conversion. The sum frequency signal generated was collected by a 100 mm lens, separated by spatial filters, and dispersed by a prism. The spectrally separated signal was then focused onto the slit (<0.5 mm) of a monochromator (Jobin Yvon, H 20 UV) and detected by a photomultiplier tube (Hamamatsu) in combination with a Stanford Research photon counter unit (SR400). Gated counting of the signal was achieved in combination with a light chopper (EG&G model 650) introduced in the optical path. Signals were acquired at each position of the chopper, open and closed, and the differences have been plotted. The upconverted fluorescence signal at different fluorescence wavelengths was detected by rotating the SFG crystal and the dispersing prism and selecting the desired wavelength with the monochromator. Pump wavelength was stopped by introducing suitable cutoff filters (Hoya filters L-42, Y-44, or Y-50) before the SFG crystal. A U-33 filter (Sigma Koki) was placed in front of the monochromator, which mainly passes the wavelength region 200–400 nm. Typical optical density at the excitation wavelength was <0.6 . During the measurement, the sample solutions were flowed through a cell of 1 mm thickness to avoid any sample heating or photodecomposition. Fresh samples were used after every 3–4 h of exposure, but no significant changes were seen in the ground-state absorption spectrum after the exposure. The excitation power at the sample was kept at 10 mW. No excitation power dependence was observed on the transient decay. The lower levels of the signal intensities were of 20–30 counts per second at the experimental conditions mentioned (vide infra). The instrument response function was obtained by upconverting the residual pump wavelength and the gate pulse. The upconverted response function fitted best to a Gaussian profile with fwhm ~ 150 fs. This has been verified separately by upconverting the Raman scattered signal from water.

Laser-excited fluorescence measurements were done with an arrangement designed to collect the fluorescence after laser excitation and focus it onto a CCD. The excitation wavelength was fixed at 405 nm, obtained from a homemade cavity-dumped mode-locked Ti:sapphire laser with the frequency set at 330 kHz (1 mW). This low repetition avoided the accumulation of long-lived triplet states having a lifetime on the order of a few hundred nanoseconds. Fluorescence emission was collected by cassegrainian optics, and additional cutoff filters were used to filter out the scattered light reaching the detector. Background light has been subtracted by accumulating under identical conditions with only solvent in the sample cell.

Results and Discussion

(i) Steady-State Measurements. Figure 1A represents the absorption and emission spectra of $[\text{Ru}(\text{bpy})_3]^{2+}$ dissolved in acetonitrile solvent. The broad, strong visible absorption of $[\text{Ru}(\text{bpy})_3]^{2+}$ ($\epsilon_{450 \text{ nm}} \approx 14\,000 \text{ dm}^3 \text{ mol}^{-1} \text{ cm}^{-1}$) is well described as a metal-to-ligand charge-transfer transition where an electron is promoted from the metal-centered t_{2g} orbital into a ligand-centered π^* orbital.¹⁹ The emission is readily obtained at ambient temperature and generally attributed to a $^3(\text{MLCT})$ state with an electron localized on one of the bipyridine rings. The failure to detect any emission on the higher energy side of the triplet-state emission (500 nm region) using the conventional fluorimeter indicates that the emission yield in this region could

(35) Caspar, J. V.; Meyer, T. J. *J. Am. Chem. Soc.* **1983**, *105*, 5583.

(36) Van Houten, J.; Watts, R. J. *Inorg. Chem.* **1978**, *17*, 3381.

(37) Van Houten, J.; Watts, R. J. *J. Am. Chem. Soc.* **1976**, *98*, 4853.

(38) Damrauer, N. H.; McCusker, J. K. *Inorg. Chem.* **1999**, *38*, 4268.

(39) (a) Shah, J. *IEEE J. Quantum Electron.* **1988**, *24*, 276. (b) Kahlow, M. A.; Jarzeba, W.; DuBruil, T. P.; Barbara, P. F. *Rev. Sci. Instrum.* **1988**, *59*, 1098.

(40) Elliott, C. M.; Hershenhart, E. J. *J. Am. Chem. Soc.* **1982**, *104*, 7519.

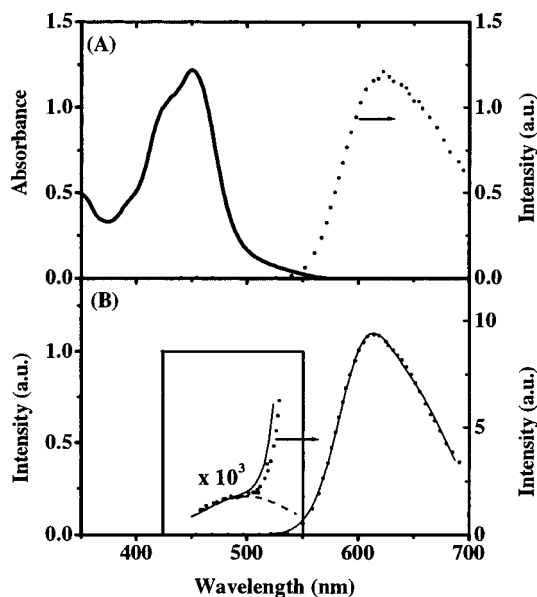


Figure 1. (A) Steady-state absorption (—) and emission (···) spectra of $[\text{Ru}(\text{bpy})_3]^{2+}$ in acetonitrile solution. (B) Emission spectrum of $[\text{Ru}(\text{bpy})_3]^{2+}$ in acetonitrile solution recorded by laser excited fluorescence measurement (···); the superimposed thin line (—) represents the fitting generated by multiple Gaussian fits. [The inset of (B) shows the 500 nm region on a magnified scale, showing the band shape in the 500 nm region]. (See also ref 41.)

have an upper limit of $\sim 10^{-4}$. Hence, we attempted to accumulate the emitted photons using CCD in a laser-excited fluorescence setup. The emission spectrum recorded using this method in an acetonitrile solution of $[\text{Ru}(\text{bpy})_3]^{2+}$ on excitation at 405 nm is shown in Figure 1B. Care has been taken to eliminate the scattered and residual pump wavelengths. Also, the background signal has been obtained under identical conditions with only the solvent in the sample cell and subtracted to get the actual spectrum.⁴¹ The presence of a weak spectral band in the 500 nm region is clearly demonstrated in the spectrum shown in Figure 1B. A similar detection method has been used to record extremely weak emission in some proton-transfer systems.⁴² To get an estimate of the emission quantum yield from the $^1(\text{MLCT})$ state, the fluorescence spectrum was fitted with multiple Gaussian profiles (see Figure 1B), and the area under the curve in the 500 nm region was compared to that of the main band. Taking $^3(\text{MLCT})$ state emission yield in acetonitrile at room temperature as 0.0642,³⁵ the $^1(\text{MLCT})$ state emission yield was evaluated to be 9×10^{-5} . This value would represent the upper limit, as it is difficult to single out any specific emitting species in this region (vide infra), and is within the upper limit of 10^{-4} predicted for this complex.^{34b}

(ii) Time-Resolved Measurements. Having obtained spectral indication for an emitting species in the 500 nm region, time-dependent emission signals were recorded by fluorescence upconversion for $[\text{Ru}(\text{bpy})_3]^{2+}$ dissolved in acetonitrile on excitation at 410 nm. The fluorescence decay traces obtained at 500, 575, and 620 nm are shown in Figure 2. The signals display an ultrafast decay (instrument limited) at ~ 500 nm, whereas rise and slower decay profiles have been observed on moving to longer wavelengths. As mentioned in the Introduction,

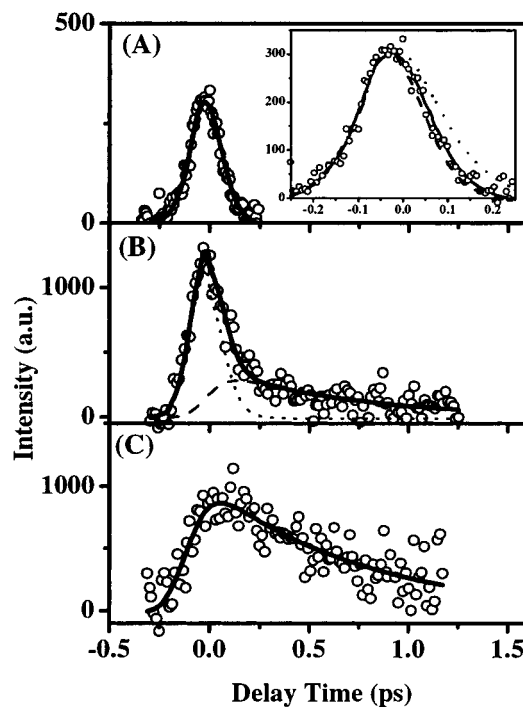


Figure 2. Fluorescence upconversion signal of $[\text{Ru}(\text{bpy})_3]^{2+}$ in acetonitrile solution (O) at (A) 500, (B) 575, and (C) 620 nm. The thick solid lines represent the fit generated by convoluting the instrument response function and exponential decay and rise functions at each wavelength. The thin dotted and dashed lines represent the individual components generated for the fit. [The inset of Figure 2A shows the convolution fitting generated with 25 (---), 40 (—), and 75 fs (···) decay times. The fit with 40 ± 15 fs is adjudged as the best-fit value.]

we do not expect any time-resolved upconverted signal from the $^3(\text{MLCT})$ states at the time scales of the experiments. Care has been taken to ensure that the ultrafast decay signal does not appear from any experimental artifacts (see Experimental Section). Since no Raman bands have been reported for this complex and the monitored wavelengths are quite far from the excitation wavelength ($\Delta\nu = 4390 \text{ cm}^{-1}$), the contribution from Raman scattering can be neglected.^{43–46} Blank experiments using only the solvent under identical conditions did not show any signal, confirming the authenticity of the ultrafast excited-state $^1(\text{MLCT})$ emission features presented here.

The fluorescence decay obtained at 500 nm (Figure 2A) is quite similar to the cross-correlation trace, indicating that a major portion of the fluorescence vanishes with a time constant much shorter than the instrument response time resolution. The decay trace, $F(t)$, was fitted by convolution of the instrument response function, $g(t)$, with a decay function, $f(t)$, which is a single-exponential function (eqs 1 and 2):

$$F(t) = \int_{-\infty}^t g(t') f(t - t') dt', \quad (1)$$

where

$$f(t) = A_1 \exp(-t/\tau_1) \quad (2)$$

(41) Since the spectral response in the Hitachi fluorimeter was corrected only up to 600 nm, there is a slight mismatch between the fluorescence spectra obtained by the two methods above 600 nm.

(42) Chou, P. T.; Chen, Y. C.; Yu, W. S.; Chou, Y. H.; Wei, C. Y.; Cheng, Y. M. *J. Phys. Chem. A* **2001**, *105*, 1731.

(43) Forster, M.; Hester, R. E. *Chem. Phys. Lett.* **1981**, *81*, 42.

(44) Bradley, P. G.; Kress, N.; Hornberger, B. A.; Dallinger, R. F.; Woodruff, W. H. *J. Am. Chem. Soc.* **1981**, *103*, 7441.

(45) Carroll, P. J.; Brus, L. E. *J. Am. Chem. Soc.* **1987**, *109*, 7613.

(46) Strommen, D. P.; Mallick, P. K.; Danzer, G. D.; Lumpkin, R. S.; Kincaid, J. R. *J. Phys. Chem.* **1990**, *94*, 1357.

The thick solid lines in Figure 2A represent the traces generated by convolution fitting, which gives 40 fs as the decay time in acetonitrile at 500 nm. Though the evaluation of decay time constant is limited by the system response function, the fits generated with 25 and 75 fs time constants are clearly distinguishable from the one with a 40 fs time constant and are shown in the inset of Figure 2A. Similar assessments have been made by several groups for different systems with instrument resolution $\sim 150\text{--}190$ fs.^{9,47} From the above analysis, the decay time constant for the ultrafast fluorescing FC state of $[\text{Ru}(\text{bpy})_3]^{2+}$ in acetonitrile is evaluated to be 40 ± 15 fs.

As mentioned earlier, wavelength-dependent kinetic changes have been observed on moving toward the spectral region where the triplet-state emission is seen. The traces recorded at 575 and 620 nm in acetonitrile solution are shown in Figure 2B and C, respectively. It was seen that, on shifting the monitoring wavelength toward longer wavelengths, the signals appeared on a constant background. These are believed to originate from the long-lived triplet state which is accumulated on excitation with the 82 MHz laser. Thus, the background counts have been subtracted from the signals presented here. At 575 nm, the decay consists of a fast component followed by a slower one, indicating the presence of more than one emitting state. Assuming a cascade population relaxation for the emitting states, the fitting analysis of the observed emission decays was carried out on the basis of the following functional form, $f(t)$, in eq 1:

$$f(t) = A_1 \exp(-t/\tau_1) + A_2[\exp(-t/\tau_2) - \exp(-t/\tau_1)] \quad (3)$$

where A_1 and A_2 represent the pre-exponential factors, τ_1 represents the decay of the first excited emitting state (as in eq 2), which also represents the rise of the second emitting state, and τ_2 represents the decay of the second emitting state. The convoluted fit, together with individually generated decay and rise components, is shown in Figure 2B. The faster decay component showed good agreement with the decay time obtained at 500 nm, 40 ± 15 fs, whereas the decay time for the slower component is evaluated to be 630 ± 50 fs. The kinetic profile becomes clear on changing the monitoring wavelength to 620 nm (Figure 2C). At this wavelength, the kinetic trace did not show the faster component, but it did show a fast rise and a slower decay. So the convolution fitting is done with only the second term in eq 3, i.e., rise and decay terms only. The data displayed good agreement with the convoluted decay profile generated with a rise time constant of 40 ± 15 fs and a decay constant of 600 ± 50 fs. Results obtained at selected wavelengths in propionitrile solution also showed kinetic behavior similar to that obtained in acetonitrile solutions. The emission time profiles obtained at 525 and 620 nm in propionitrile solution are shown in Figure 3, together with the fitted curves. At 525 nm the decay fits to eq 3, which gives the faster decay time as 40 ± 15 fs and the slower one as 560 ± 40 fs. At 620 nm, the decay conformed to a rise and decay function with values of 40 ± 15 and 580 ± 70 fs, respectively.

In alcoholic solutions, the contribution from the slower component was greater than that observed in nitrile solutions. This is evident from Figure 4, which shows the traces obtained at 500 and 575 nm in methanol, ethanol, and 1-propanol solutions. In methanol solutions (Figure 4A), the decay at 500

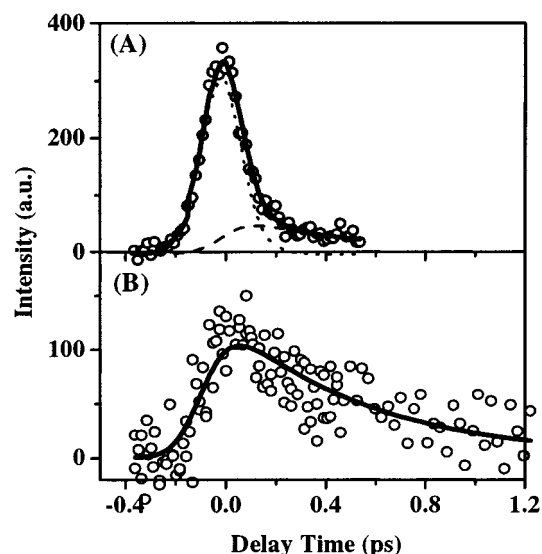


Figure 3. Fluorescence upconversion signal of $[\text{Ru}(\text{bpy})_3]^{2+}$ in propionitrile solution (\circ) at (A) 525 and (B) 620 nm. The thick solid lines represent the fit generated by convoluting the instrument response function and exponential decay and rise functions at each wavelength. The thin dotted and dashed lines represent the individual components generated for the fit.

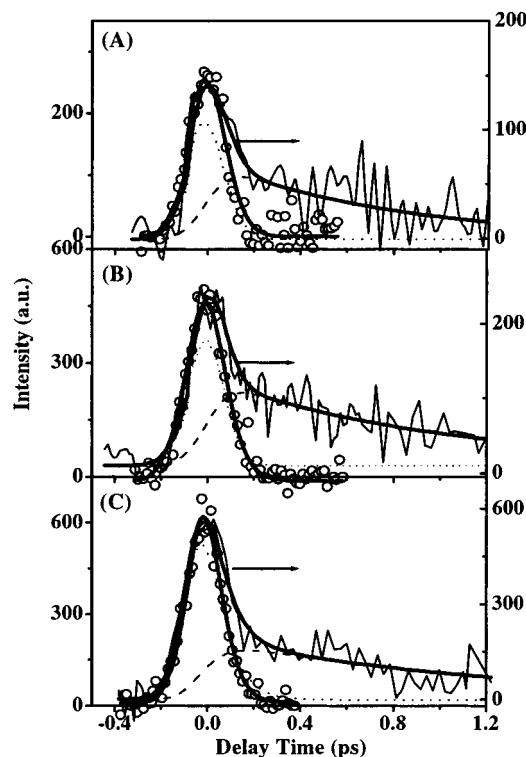


Figure 4. Fluorescence upconversion signal of $[\text{Ru}(\text{bpy})_3]^{2+}$ in methanol (A), ethanol (B), and 1-propanol (C) solutions. Open circles (\circ) represent the signal obtained at 500 nm, and thin lines ($-$) represent the signal recorded at 575 nm. The thick solid lines represent the best convolution fitting, and the thin dotted and dashed lines represent the individual components generated for the fit.

nm gave a good fit with a single decay time of 40 ± 15 fs, whereas at 575 nm, the biexponential decay conformed to eq 3, with the slower component as 800 ± 150 fs and the faster one representing the kinetics at 500 nm. The convolution fitting to these data has been presented in Figure 4A. In ethanol solutions, the decay at 500 nm is best fitted with a decay time of 40 ± 15 fs, and at 575 nm the kinetic analysis gives values

(47) Takeuchi, S.; Tahara, T. *J. Phys. Chem. A* **1997**, *101*, 3052.

Table 1. Decay Constants Evaluated by Fluorescence Upconversion Measurements on $[\text{Ru}(\text{bpy})_3]^{2+}$ in Different Solvents at Different Wavelengths on Excitation at 410 nm

solvent	thermal diffusivity ^a (10^{-7} m ² /s)	time constants		
		measured at 500 nm	measured at 575 nm ^b	measured at 620 nm
methanol	0.998	$\tau_1 = 40 \pm 15$ fs	$\tau_1 = 40 \pm 15$ fs $\tau_2 = 800 \pm 150$ fs	
ethanol	0.878	$\tau_1 = 40 \pm 15$ fs	$\tau_1 = 40 \pm 15$ fs $\tau_2 = 1.0 \pm 0.12$ ps	
propanol	0.800	$\tau_1 = 40 \pm 15$ fs	$\tau_1 = 40 \pm 15$ fs $\tau_2 = 1.3 \pm 0.18$ ps	
acetonitrile	1.075	$\tau_1 = 40 \pm 15$ fs	$\tau_1 = 40 \pm 15$ fs $\tau_2 = 630 \pm 50$ fs	$\tau_r = 40 \pm 15$ fs ^d $\tau_2 = 600 \pm 50$ fs
propionitrile			$\tau_1 = 40 \pm 15$ fs ^c $\tau_2 = 560 \pm 40$ fs ^c	$\tau_r = 40 \pm 15$ fs ^d $\tau_2 = 580 \pm 70$ fs

^a Values taken from ref 54. ^b At this wavelength, τ_1 also represents the rise time constant. ^c The kinetics have been obtained at 525 nm. ^d τ_r represents the rise time constant.

40 ± 15 fs and 1.0 ± 0.12 ps for the rise and decay constants, respectively. The data along with the fitted curves are shown in Figure 4B. Similar analyses have been carried out on the data obtained from 1-propanol solutions (Figure 4C). The fit gave 40 ± 15 fs as the decay constant at 500 nm and 40 ± 15 fs and 1.3 ± 0.18 ps as the rise and decay components respectively at 575 nm. The kinetic parameters obtained in different solvents have been tabulated in Table 1. It should be mentioned here that we could not detect any signal at 620 nm in the alcoholic solutions, probably because it is too weak to be detected.

The ³(MLCT) state is reported to have a formation time of ~ 100 fs on excitation at 480 nm in different solvents.^{30,32} The results obtained in the present case on excitation at 410 nm show that the average time constant obtained at shorter wavelengths in different solvents corresponds to 40 ± 15 fs. Though the transient absorption and fluorescence decay measurements would provide information on the excited-state properties, the studies on the triplet absorption characteristics reported earlier are a more general assessment of how long it takes for the ³(MLCT) to become established in terms of its absorptive properties.^{30,32} On the other hand, fluorescence measurements are more discriminating and would reveal the time constant with respect to when the wave function evolves from predominantly singlet to triplet character, i.e., intersystem crossing (ISC). Thus, the decay time constant reported here, 40 ± 15 fs, and the triplet state formation time, 100 fs, reported McCusker and co-workers^{30,32} have to be seen on the basis of the above two aspects. Possible assignment of the fast and slow decays to a fast internal conversion (IC) and a subsequent ISC from the relaxed ¹(MLCT) state, respectively, is considered. However, on the basis of the reported triplet state rise time and the fact that no significant absorption changes were found in the triplet–triplet absorption spectra after a delay of ~ 300 fs,^{30,32} it is probable that the slower component (which is in the 0.56–1.3 ps range) does not represent any process from the relaxed S_1 state. On the other hand, excited-state dynamics of ruthenium complexes has been shown to be excitation wavelength dependent, which has been attributed mainly to the presence of a large number of spin–orbit coupled states above the first excited singlet state.^{25,30,32,37} It is to be noted here that the presence of a Ru atom will have a dominant role in the spin crossover process. Thus, it is reasonable to attribute the 40 ± 15 fs time constant observed on excitation by a 410 nm pulse to the ISC

process from the higher excited ¹(MLCT) state of $[\text{Ru}(\text{bpy})_3]^{2+}$. Significant interaction between the ruthenium metal d orbitals and the ligand π^* orbitals results in a large spin–orbit coupling, and this is believed to be the driving force for such an ultrafast ISC process. It has been a long-standing problem to accurately evaluate the lifetime of the FC singlet state in $[\text{Ru}(\text{bpy})_3]^{2+}$. Though recent pump–probe measurements on the evolution of the triplet state have been successful to some extent, to the best of our knowledge the results herein present the first report on direct observation of the emissive FC singlet state and the ISC time constant of $[\text{Ru}(\text{bpy})_3]^{2+}$ in the solution phase.^{30,32}

The rise and decay kinetics observed on monitoring in the wavelength region of triplet emission has been examined on the basis of dynamic Stokes' shift and/or vibrational relaxation. In the former case, the rise component observed at longer wavelength could be seen as originating from a dynamic Stokes' shift. However, the rise time obtained for the faster component (40 ± 15 fs) in different solvents did not show a dependence on the solvent. Moreover, in such a case, the slower decay component (ranging from 0.56 to 1.3 ps) evaluated in different solvents is attributed to the decay of the solvated S_1 state, which is not consistent with the existing data.^{30,32} Thus, it is quite unlikely that the kinetic profiles mentioned above represent any dynamic Stokes' shift governed by environmental forces such as solvation. However, it becomes difficult to preclude its contribution to the rise and decay kinetics observed here.

In the latter case, the kinetics has been viewed as relaxation from higher excited singlet/triplet states. Damrauer et al. reported biexponential decay kinetics with lifetimes of 120 ± 40 fs and 2–5 ps for methyl/benzyl-substituted derivatives of $[\text{Ru}(\text{bpy})_3]^{2+}$ on excitation at 400 nm using transient absorption measurements.⁴⁸ The faster decay, which was instrument limited, has been assigned to the ISC process, whereas the slower one has been assigned to a vibrational cooling in the triplet manifolds. Damrauer et al. also observed analogous decay kinetics for the $[\text{Ru}(\text{bpy})_3]^{2+}$ system, but no decay constant has been reported. Variable-temperature emission studies carried out for a series of substituted bipyridyl and polypyridyl complexes of Ru(II) have shown vibrational features with considerable blue shift on lowering the temperature.^{38,49} Further, the temperature dependence of the emission lifetime and quantum yield studies has

(48) Damrauer, N. H.; McCusker J. K. *J. Phys. Chem. A* **1999**, *103*, 8440.

(49) DeArmond, M. K.; Carlin, C. M. *Coord. Chem. Rev.* **1981**, *36*, 325.

revealed the presence of a large number of spin-orbit coupled states, within $\sim 3000\text{ cm}^{-1}$ of the lowest excited levels, which would contribute to the overall decay process of $[\text{Ru}(\text{bpy})_3]^{2+}$.³⁷ Considering these aspects, it is believed that the fast ISC from the higher $^1(\text{MLCT})$ state is efficient in releasing the excitation energy into the higher vibrational levels in the triplet manifold, which are emissive. Thus, the slow decay component observed in the decay kinetics could be safely assigned to a relaxation from vibrationally excited triplet states, i.e., vibrational cooling in the triplet manifold. Also, the observation that the time-resolved fluorescence traces obtained above 525 nm appeared on a constant background count (which has been subtracted from the traces shown here) is a clear indication that the relaxation would eventually populate the long-lived relaxed $^3(\text{MLCT})$ state. Though the slow decay could as well represent an electronic relaxation in the triplet, a meaningful discussion on this topic requires experimental data from excitation wavelength-dependent studies. In a broad view, rather than dealing with two distinct emission profiles, the data may correspond to a continually evolving spectrum, the precise analysis of which requires more accurate experimental data.⁵⁰

It is already established that the emission from the relaxed triplet state is long-lived and the radiative rate constant (k_r) is not sufficient to give the upconversion signal. However, this need not be the case with the higher lying states in the triplet. As mentioned earlier, it could be a factor of the extent to which the interaction of the metal d orbitals and the ligand π orbitals results in pronounced spin-orbit coupling. Mixing in the vibronic levels of singlet and triplet characteristics in the transition metal complexes has been discussed in detail from various experimental point of view.⁴⁹ In other words, mixing of the higher levels in the triplet state with the singlet state would enhance the k_r of the vibrationally hot states within the triplet manifold, facilitating the upconversion of the emitted photons. This explanation needs to be considered in parallel with the earlier suggestion, which precludes the possibility that there is any well-defined establishment of the wave packet on any potential energy surface other than the lowest energy $^3(\text{MLCT})$ state in the course of excited-state relaxation.³² The anomaly that the longest detection wavelength (620 nm) at which the emission from the vibrationally hot state observed is near the relaxed triplet emission maximum is understood to be due to a favorable Franck-Condon factor for the hot band-to-hot band emission between the two electronic states; i.e., transitions occur from numerous higher vibronic levels in the triplet manifold to the higher states in S_0 during the vibrational relaxation and later on from the lower levels in the triplet manifold to lower vibrational levels in S_0 .^{51,52} The presence of such vibrational levels in the ground state of $[\text{Ru}(\text{bpy})_3]^{2+}$ and the contribution of individual vibrational levels of the ground state to the overall steady-state emission spectrum have been demonstrated in a Franck-Condon analysis of the emission spectrum.^{27,53} So, it is not surprising that the hot band emissions are broader and

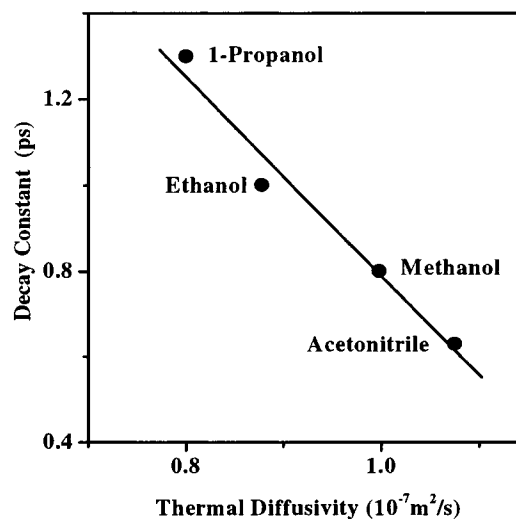


Figure 5. Plot of vibrational cooling time constant in $[\text{Ru}(\text{bpy})_3]^{2+}$ (slower component in the emission decay) versus the thermal diffusivity of the solvent.

diffused. It should be mentioned here that, since the excitation energy is quite high in the singlet state, there is a possibility of a competition between the ISC and relaxation to the lowest singlet state. Such a situation would result in a continuously evolving spectral profile, but as mentioned earlier, a meaningful discussion on this point requires experimental data at different excitation wavelengths.

The decay time of the vibrational cooling has been found to vary from solvent to solvent (Table 1). Considering the uncertainties associated with the decay constants obtained from such low-intensity signals, it becomes difficult to make any conclusive assignment of the solvent effect observed on the decay constant presented here. However, on a qualitative basis, a correlation with some of the solvent parameters has been examined. Intermolecular transfer of excess vibrational energy to a solvent molecule has been studied for a number of molecules under a variety of conditions where the dependence of the lifetime of a vibrationally excited molecule on a specific solvent is well correlated with the thermal diffusivity of the solvent.⁵¹ An attempt has been made to find any correlation of the vibrational cooling time, i.e., the slower decay time, with the thermal diffusivity of the solvents. A plot of observed vibrational cooling time versus the thermal diffusivity of the solvents is presented in Figure 5.⁵⁴ The good linear relationship displayed provides added support to the conclusion that the slower decay component originates from a vibrationally excited triplet state. At this stage, one can consider the solvation of the excited state by the solvent molecule affecting the decay times. However, this possibility is quite low since the characteristic decay times obtained for the solvents used, e.g., acetonitrile, methanol, ethanol, and propanol ($\sim 0.6, 0.8, 1.0,$ and 1.3 ps, respectively) are far from the relaxation times reported for these solvents.⁵⁵

An interligand electron-transfer model has been put forward to explain the difference in the relaxation dynamics of RuN3

(50) A detailed analysis requires complete spectra to carry out a single-valued decomposition analysis of the data. A two-spectrum model will yield two eigenvalues, whereas a continuously evolving spectrum will yield far more than two.

(51) Kaiser, W., Ed. *Ultrashort Laser Pulses and Applications*; Springer-Verlag: Berlin, Heidelberg, 1988; Chapter 7.

(52) Ermolaev, V. L. *Russ. Chem. Rev.* **2001**, *70*, 471.

(53) Hartman, P.; Leiner, M. J. P.; Draxler, S.; Lippitsch, M. E. *Chem. Phys.* **1996**, *207*, 137.

(54) Bialkowski, S. E. *Photothermal spectroscopy methods for chemical analysis*; Chemical Analysis: A series of monographs on analytical chemistry and its applications, Vol. 134; Winefordner, J. D., Ed.; John Wiley & Sons: New York, 1996.

(55) Horng, M. L.; Gardecki, J. A.; Papazyan, A.; Maroncelli, M. *J. Phys. Chem.* **1995**, *99*, 17311.

dye in solvents such as methanol and acetonitrile.²⁵ A similar model has also been proposed to hold in explaining the observed solvent effects observed for the $[\text{Ru}(\text{bpy})_3]^{2+}$ system.²⁵ However, this model, mainly concerned with the relaxation process in the long-lived ³(MLCT) states, would not be significant in explaining the solvent effects observed in the present work. It may be mentioned here that our ongoing studies on the ultrafast emission properties of RuN3 dye in some selected solvents also yielded fluorescence decay signals (monitored at ~ 625 nm) similar to that seen at 500 nm in the present case. Unlike $[\text{Ru}(\text{bpy})_3]^{2+}$, RuN3 triplet is nonemissive at room temperature, and we hope that our ongoing studies on different metal complexes will bring out more information on the vibrational hot states and/or solvation processes in these systems.

In the band-selective sensitization studies of TiO_2 by $\text{Fe}(\text{dcbp})_2(\text{CN})_2$, it has been reported by Ferrere and Gregg that while electron injection is relatively efficient (10–11%) from the higher energy MLCT state (~ 420 nm), injection is much less efficient ($\sim 2\%$) from the lower energy MLCT transition (~ 600 nm).¹⁵ This indicates that dynamics in the higher energy excited states is of crucial importance in understanding the overall electron injection process. It has been shown by Benko et al. that the dominating part of the electron transfer proceeds extremely rapidly from the initially populated, vibronically nonthermalized singlet excited state, prior to electronic and nuclear relaxation of the molecule.¹³ Evidence for the electron injection from the higher excited state has also been reported when the LUMO of the dye sensitizer is below the conduction band of the semiconductor nanoparticle.¹⁷ These reports confirm that the time scales for the ultrafast electron injection dynamics need to be examined in relation to various excited-state processes in the sensitizer dyes, namely, IC, ISC, vibrational relaxation, solvation, structural rearrangement, etc. This work presents the relaxation dynamics involving the higher excited state in $[\text{Ru}(\text{bpy})_3]^{2+}$, provides first-hand information on the ISC time constant and relaxation pathways in these systems, and underlines the importance of “active” higher excited levels in the singlet and triplet MLCT states in explaining the overall photochemistry of a metal complex system.

In conclusion, the excited-state dynamics of a transition metal complex, $[\text{Ru}(\text{bpy})_3]^{2+}$, has been investigated using femtosecond

fluorescence upconversion spectroscopy. Emission from the Franck–Condon excited singlet state of $[\text{Ru}(\text{bpy})_3]^{2+}$ has been observed for the first time, and its lifetime has been adjudged to be 40 ± 15 fs. Biexponential decay with a fast rise component observed at longer wavelengths indicated that there was more than one emitting state in the system. The slower component, which grew concomitant with the decay of the ¹(MLCT) state, displayed decay constants in the range of 0.56–1.3 ps in different solvents studied. It has been proposed that, on excitation at 410 nm, crossover from a higher excited ¹(MLCT) state to a vibrationally hot triplet manifold occurs with an ISC time constant of 40 ± 15 fs. Mixing of the higher levels in the triplet state with the singlet state is believed to enhance the k_r of the vibrationally hot states within the triplet manifold, facilitating the upconversion of the emitted photons. The vibrationally excited triplet, which is emissive, undergoes vibrational cooling and relaxes to the long-lived triplet state. The results on the relaxation dynamics of the higher excited states in $[\text{Ru}(\text{bpy})_3]^{2+}$ are valuable in explaining the role of nonequilibrated higher excited sensitizer states of transition metal complexes in the electron injection and other ultrafast processes.

Acknowledgment. The authors are grateful to the reviewers for their critical comments and valuable suggestion which helped in improving the manuscript. A.C.B. gratefully acknowledges the postdoctoral financial support provided by the Japan Society for Promotion of Science (P 99280) for carrying out of this research project. A.C.B. takes this opportunity to thank all members in the laboratory of Prof. Okada for providing fruitful discussions and constant help throughout this work. A.C.B. thanks Dr. A. V. Sapre of Bhabha Atomic Research Centre for critically going through the manuscript and providing valuable suggestions and acknowledges the permission given by Bhabha Atomic Research Centre to carry out postdoctoral research in Japan. The work was also supported by a Grant-in-Aid for Specially Promoted Research (No. 10102007) from the Ministry of Education, Sports and Culture, Science and Technology, Japan.

JA026135H